

## Research Paper

# Jujuboside A promotes A $\beta$ clearance and ameliorates cognitive deficiency in Alzheimer's disease through activating Axl/HSP90/PPAR $\gamma$ pathway

Mu Zhang<sup>1, #</sup>, Cheng Qian<sup>1, #</sup>, Zu-Guo Zheng<sup>1</sup>, Fei Qian<sup>1</sup>, Yanyan Wang<sup>1</sup>, Pyone Myat Thu<sup>1</sup>, Xin Zhang<sup>1</sup>, Yaping Zhou<sup>1</sup>, Lifan Tu<sup>1</sup>, Qingling Liu<sup>1</sup>, Hui-Jun Li<sup>1</sup>, Hua Yang<sup>1</sup>, Ping Li<sup>1</sup>✉ & Xiaojun Xu<sup>1, 2</sup>✉

1. State Key Laboratory of Natural Medicines, China Pharmaceutical University, 210009, Nanjing, Jiangsu, China
2. Jiangsu Key Laboratory of Metabolic Disease, China Pharmaceutical University, 210009, Nanjing, Jiangsu, China

#These authors contributed equally to this work.

✉ Corresponding authors: Ping Li, PhD, Department of Pharmacognosy, China Pharmaceutical University; 24 Tongjia Lane, Nanjing 210009, China. Tel./Fax: +86 25 83271379; E-mail: liping@cpu.edu.cn; Xiaojun Xu, PhD, Associated Professor, 24 Tongjia Lane, Nanjing 210009, China. Tel./Fax: +86 25 83271379; E-mail: xiaojunxu@cpu.edu.cn.

© Ivyspring International Publisher. This is an open access article distributed under the terms of the Creative Commons Attribution (CC BY-NC) license (<https://creativecommons.org/licenses/by-nc/4.0/>). See <http://ivyspring.com/terms> for full terms and conditions.

Received: 2018.03.19; Accepted: 2018.07.03; Published: 2018.07.30

## Abstract

**Rationale:** It has been reported that peroxisome proliferator activated receptor  $\gamma$  (PPAR $\gamma$ ) level decreases significantly in the brains of Alzheimer's disease (AD) patients and mice models, while the mechanism is unclear. This study aims to unravel the mechanism that amyloid  $\beta$  (A $\beta$ ) decreases PPAR $\gamma$  and attempted to discover lead compound that preserves PPAR $\gamma$ .

**Methods:** In APP/PS1 transgenic mice and A $\beta$  treated microglia, the interaction between HSP90 and PPAR $\gamma$  were analyzed by western blot. Using a PPRE (PPAR $\gamma$  responsive element) containing reporter cell line, compounds that activate PPAR $\gamma$  activity were identified. After genetic ablation or pharmacological inhibition of potential target pathways, the target of jujuboside A (JuA) was discovered through Axl/HSP90 $\beta$ . After oral administration or intrathecal injection, the anti-AD activity of JuA was evaluated by Morris water maze (MWM) test and object recognition test. Soluble A $\beta$ 42 levels and plaque numbers after JuA treatment were detected by thioflavin S staining, and the activation of microglia was assayed by immunofluorescence staining against Iba-1.

**Results:** We found that A $\beta$  stress decreased heat shock protein 90  $\beta$  (HSP90 $\beta$ ), subsequently reduced the abundance of PPAR $\gamma$ , and down-regulated A $\beta$  clearance-related genes in BV2 cells and primary microglia. We identified that JuA stimulated the expression of HSP90 $\beta$ , strengthened the interaction between HSP90 $\beta$  and PPAR $\gamma$ , preserved PPAR $\gamma$  levels, and thus effectively promoted the clearance of A $\beta$ 42. We demonstrated that JuA increased HSP90 $\beta$  expression through Axl/ERK pathway. JuA significantly ameliorated cognitive deficiency in APP/PS1 transgenic mice, meanwhile, JuA significantly reduced the soluble A $\beta$ 42 levels and plaque numbers in the brain. Notably, the therapeutic effects of JuA were dampened by R428, an Axl inhibitor.

**Conclusions:** This study suggests that the up-regulation of HSP90 $\beta$  by JuA through Axl is a potential therapeutic strategy to facilitate A $\beta$ 42 clearance and ameliorate cognitive deficiency in AD.

Key words: Alzheimer's disease, amyloid  $\beta$ , Jujuboside A, PPAR $\gamma$ , HSP90 $\beta$ , Axl

## Introduction

Accumulation of senile plaques in brain tissue is one of the main pathological features of AD [1]. A $\beta$ 42 is the primary component of the senile plaques [2], which induces a series of pathological changes including chronic inflammatory reaction, oxidative injury, tangles formation and progressive synaptic injury [3, 4]. Despite significant efforts to develop

treatments, the field has seen little success, partially due to an incomplete understanding of the mechanisms underlying disease pathogenesis [5]. A $\beta$  deposition could start years or even decades before the appearance of dementia symptoms [6]. Notably, late onsets AD patients exhibit compromised A $\beta$  clearance rather than over production of A $\beta$  [7], and

thus promoting A $\beta$  clearance becomes an attractive strategy in AD treatment.

Microglia are the only type of resident macrophages in the central nervous system (CNS) [8, 9]. Activated microglia uptake soluble or fibrillar A $\beta$  and degrade these peptides through proteasome pathways [10, 11]. The abnormal increase of soluble A $\beta$  level could be attributed to either increased A $\beta$  production or decreased A $\beta$  clearance, in many cases, both [4, 12]. Microglia lose their phagocytic activity gradually during the progression of AD [13, 14], and this process is also highly sensitive to inflammatory stimuli [15, 16]. Emerging evidences suggest that PPAR $\gamma$  effectively regulates the activation of microglia under physiological and pathological conditions, and is recognized as a therapeutic target for AD [17, 18]. Firstly, PPAR $\gamma$  activation enhances microglia phagocytosis of soluble A $\beta$  and insoluble deposits [9, 19]. Secondly, PPAR $\gamma$  induces the expression of *ApoE*, *ABCA1* and *ABCG1*; hence, it increases lipidated ApoE levels and facilitates the degradation of soluble A $\beta$  peptides by microglia [9, 12, 19]. It is worth noting that in the brains of APPV717I transgenic mice and AD patients, the PPAR $\gamma$  level decreases significantly [20]. As a consequence, A $\beta$  clearance capacity decreases and the progression of AD is subsequently exacerbated. However, the mechanism of how PPAR $\gamma$  is decreased in AD patients remains largely elusive.

HSP90 is an evolutionarily conserved molecular chaperone that is essential for the folding, maturation and stability of several hundreds of client proteins, including thermodynamically unstable proteins, kinases and nuclear receptors. In aged individuals, the damaged proteins accumulate, which leads to an increase in chaperone occupancy. The function and content of HSP90 were found to be greatly impaired in old animals [21], as well as in patients with early or late onset AD or mild cognitive impairment [22]. In AD animal models, overexpression of molecular chaperones, including HSP90, suppresses the early stages of self-assembly [23, 24], and thus pharmacological activation of chaperones might have a favorable therapeutic effect on AD. It has been reported that, under stressed conditions, or when HSP90 function is blocked, PPAR $\gamma$  is depleted in the detergent-soluble fraction and sediments in the detergent-insoluble pellets, which leads to loss of its proper structure and function in 3T3-L1 cells [25, 26]. However, the relationship between AD progression and HSP90/PPAR $\gamma$  has not been completely elucidated in neurodegenerative diseases.

Given the facts above, we hypothesized that chronic A $\beta$  exposure leads to HSP90 function impairment, which inactivates PPAR $\gamma$  and decreases

A $\beta$  clearance capacity in microglia. Compounds that promote the expression of HSP90 in microglia revive PPAR $\gamma$  activity, as well as A $\beta$  clearance capacity, and thus delay the progression of AD.

Jujuboside A (JuA) is a triterpene saponin isolated from Semen Ziziphi Spinosae. JuA has been reported to have several biological activities including anti-oxidant, anti-inflammation, anti-apoptosis and neuro-protection [27-29]. In the present study, we demonstrated that JuA significantly restored the content and function of PPAR $\gamma$  in BV2 cells and primary microglia through enhancing the expression of HSP90 $\beta$ . JuA treatment effectively promoted A $\beta$ 42 clearance by microglia and ameliorated cognitive deficiency in AD mice models. In addition, we identified that JuA upregulated the expression of HSP90 $\beta$ , at least in part, due to activating ERK through Axl receptor tyrosine kinase.

## Methods

### Reagents

Human A $\beta$ 42 peptides were purchased from ChinaPeptides (Suzhou, China). Mouse non-target control siRNA (sc-37007), HSP90 $\beta$  siRNA (sc-35607), HSP90 $\alpha$  siRNA (sc-35609), Axl siRNA (sc-29770) were purchased from Santa Cruz (Dallas, USA). Jujuboside A (A0274) was purchased from Must Biological Technology Co. Ltd. (Chengdu, China). GW9662 (S2915), Rosiglitazone (S2556) was purchased from Selleck (Houston, USA). SCH772984 (HY-50846), Dovitinib (HY-50905), Gefitinib (HY-50895), Sunitinib (HY-10255A), LDC1267 (HY-12494), UNC2250 (HY-15797), R428 (HY-15150), CHIR-99021 (HY-10182) were purchased from MedChem Express (Shanghai, China). Stock solution of all drugs were made with DMSO (Sigma-Aldrich, St. Louis, MO, USA), and diluted in Dulbecco's modified Eagle's medium (DMEM) to final concentrations in cell experiments, or diluted in saline for animal treatment. The final concentration of DMSO is no more than 0.1%. Thioflavin S (T1892), DL-homocysteine (H4628) were purchased from Sigma-Aldrich (St. Louis, USA). The purity of each compound was determined to be higher than 98% by HPLC. DMEM, fetal bovine serum (FBS), Leibovitz's L-15 medium and penicillin/streptomycin were purchased from Gibco (New York, USA). Human A $\beta$ 42 enzyme-linked immunosorbent assay (ELISA) kit was purchase from Cusabio (Wuhan, China).

### Antibodies

Rabbit anti-PPAR $\gamma$  (A0270), HSP90 $\alpha$  (A0365), HSP90 $\beta$  (A1087), and mouse anti-GAPDH (AC002) antibodies were purchased from Abclonal (Wuhan, China). Rabbit anti-p-ERK 1/2 (4377S,

Thr202/Tyr204) and ERK 1/2 (4695S) antibodies were purchased from Cell Signaling Technology (Beverly, USA). Rabbit anti-HSP90 (ab13495), Axl (ab32828), tau (ab64193) and p-tau (ab151559, Thr231) antibodies were purchased from Abcam (Cambridge, UK). Rabbit anti-Iba-1 (019-19741) antibody was purchased from Wako (Wako, Japan). Horseradish Peroxidase (HRP)-labeled goat anti-rabbit or mouse secondary antibodies were purchased from Beyotime (Shanghai, China).

### Cell culture

BV2 cells were grown in DMEM supplemented with 6% FBS and 1% penicillin/streptomycin at isobaric oxygen in 5% CO<sub>2</sub> at 37 °C.

Primary microglia were prepared from P2 rats as previously described [30]. Briefly, P2 neonatal rats were ice-anaesthetized and decapitated. The whole brain was removed in chilled saline and then placed into Leibovitz's L-15 conditioned media (Leibovitz's L-15, 0.1% BSA, 1% penicillin/ streptomycin) on ice. After removing the meninges from the brain, the isolated cortex tissue was placed into a new Petri dish with L-15 conditioned media on ice. Tissues were dissociated through pipetting up and down with a sterile pipette and the material were dispensed through a cell strainer (100 µm pore), centrifuged (2500 ×g, 5 min, 4 °C) and resuspended with 6 mL culture media (DEME, 10% FBS, 1% penicillin/ streptomycin), then plated into T75 flasks containing 12 mL culture media. Flasks were incubated at 37 °C and 5% CO<sub>2</sub> until mixed glial cultures were completely confluent. Flasks were shaking at 100 rpm for 1 h at 37 °C. Microglia in the medium were collected and seeded into new dishes or plates with culture media.

### Preparation of Aβ<sub>42</sub> peptides

The Aβ<sub>42</sub> peptides preparation was performed as described before [31]. Lyophilized human Aβ<sub>42</sub> peptides were dissolved in hexafluoroisopropanol (HFIP) and incubated at room temperature for 30 min. Then, HFIP was removed in a speed vacuum and the peptide film was stored at -80 °C until use. For soluble oligomeric conditions, peptides were dissolved in Ham's F-12 (phenol red-free) to a final concentration of 100 µM and incubated at 4 °C for 24 h.

### Animal study

All experiments and animal care in this study were conducted in accordance with the National Institutes of Health guide for the care and use of Laboratory animals (NIH Publications No. 8023, revised 1978), and the Provision and General Recommendation of Chinese Experimental Animals Administration Legislation and approved by the

Science and Technology Department of Jiangsu Province (SYXK (SU) 2016-0011). Male APP<sup>swe</sup>/PS1Δ9 (APP/PS1) transgenic mice [B6C3-Tg (APP<sup>swe</sup>, PSEN1dE9)85Bdo/J] at 8 months of age with body weights ranging from 35 to 40 g and their wild type litter mates were obtained from Model Animal Research Center of Nanjing University. The animals were kept under a consistent temperature (24 °C) with 12 h light/dark cycle and fed with standard food pellets with access to sterile water *ad libitum* (n=10 per group). Saline (0.1% DMSO), Rosiglitazone (Rog) (0.5 mg/kg/d), JuA (0.5, 1.5 or 5 mg/kg/d) or R428 (3.5 mg/kg, 30 min before the JuA administration) + JuA (5 mg/kg/d) were administrated to the mice through intrathecal injection (i.t.) or by oral gavage once daily for 7 days.

### Drug delivery

To enhance the delivery of compounds to the CNS, we chose intrathecal injection, which is widely used in the clinic [32, 33], intrathecal injection was performed as described before [34]. The drugs were injected intrathecally (each in 10 µL) by means of lumbar puncture at the intervertebral space of L4-5 or L5-6 for multiple injections using a stainless steel needle (30 gauge) attached to a 25 µL Hamilton syringe.

### Morris water maze test

MWM test was performed to detect spatial memory as previously described [35]. The escape latencies, swimming speed, time spent in target quadrant and platform-crossing times, were recorded and analyzed by the analysis-management system (Viewer 2 Tracking Software, Ji Liang Instruments, China).

### Object recognition test

The object recognition test was performed as described before [36]. In short, the test proceeded in a square open field apparatus with a side length of 50 cm. A white cube with side length 8 cm and a blue cylinder with diameter and height of 10 cm were used as the objects to be recognized. In the habituation session, each mouse was individually placed into the empty open field, facing the wall that is near the operator, and the animal was allowed to explore the open field for 5 min, then returned to its home cage. The open field apparatus was cleaned with 70% (v/v) ethanol to minimize olfactory cues before the next mouse entered the open field. The familiarization session was performed 24 h after the habituation step. Two identical objects, either cubes or cylinders, were placed in the open field and 5 cm away from the walls. The mouse was placed in the open field with its head positioned opposite the objects. The mouse was

allowed to freely explore for 10 min and then return to its home cage. The open field and objects were cleaned with 70% (v/v) ethanol and air-dried before next use. After all of the animals completed the familiarization session, the two familiar objects were replaced, one with a triplicate copy and the other with a novel object. In the present experiments, one white cube and one blue cylinder were used in the test session. Twenty-four hours after the familiarization session, the test session was performed. The two objects were placed at the same location as before and the animals were allowed to explore freely for 2 min. The exploration time of familiar object and novel object were recorded for analysis. The discrimination index was calculated as follows: Discrimination index = (% time with novel object - % time with familiar object)/(% time with novel object + % time with familiar object) [37]

### Brian tissue preparation

After the behavior test, mice were anaesthetized by intra-peritoneal injection of pentobarbital sodium (45 mg/kg) and then perfused with phosphate-buffered saline (PBS). Brain tissues were immediately removed from the skull. For biochemical analysis, the frontal cortex and hippocampus were separated from brain tissue and stored at -80 °C until use. For thioflavine S staining and immunofluorescence assay, the whole brains were fixed in 4% paraformaldehyde overnight at 4 °C.

### Thioflavine S staining

The A $\beta$  plaques in brain tissue were detected by thioflavine S stain. The thioflavine S staining was performed as described before [38]. In brief, after overnight fixation in paraformaldehyde, brain tissues were dehydrated by 30% sucrose solution, and then cut into 20  $\mu$ m paraffin sections. 1% thioflavine S solution was prepared in distilled water and filtered. Brain tissue sections were defatted in xylene and then hydrated through a series of ethanol solutions (100%, 95%, 80%, 70%; 1 min in each solution), placed in water for a few seconds and then stained with 1% thioflavin S for 30 min at room temperature. Subsequently, the sections were dehydrated through a series of ethanol solutions (70%, 80%, 95%, 100%; 1 min in each solution) and xylene for 5 min. Then, the sections were coverslipped with neutral balsam. Thioflavin S staining sections were viewed under ultraviolet light and captured with a fluorescence microscope (Nikon Ti-S, Tokyo, Japan).

### Intracellular A $\beta$ clearance assay

The intracellular A $\beta$  clearance assay was performed as previously described [19]. Briefly, BV2 cells were pretreated with drugs for 18 h and then

administrated with 2  $\mu$ g/mL soluble A $\beta$ 42 in serum-free medium for 24 h in the presence of drugs. At the end of the treatment, cells were washed with PBS to remove remaining A $\beta$ 42 that attached on the cell surface. Then, cells were lysed by 1% SDS and the intracellular A $\beta$ 42 levels were measured by ELISA kit according to the manufacturer's instructions.

### Brain A $\beta$ 42 measurement

The cortex and hippocampus samples were lysed in RIPA buffer containing protease inhibitor (Roche, Germany). The A $\beta$ 42 levels were detected by ELISA kit and normalized by total protein concentration.

### Western blot assay

BV2 cells and primary microglia were pretreated with 1, 5 or 25  $\mu$ M JuA followed by the treatment with 5  $\mu$ M A $\beta$ 42 for 12 h. Cells were lysed on ice with RIPA buffer (50 mM Tris (pH 7.4)), 150 mM NaCl, 1% NP-40, 0.5% sodium deoxycholate, 0.1% SDS, 0.5 mM EDTA) with protease inhibitor phosphatase inhibitors (Roche, Germany). Protein samples were separated by electrophoresis using 10% sodium dodecyl sulfate polyacrylamide gel electrophoresis (SDS-PAGE) and transferred onto polyvinylidene fluoride (PVDF) membranes. Then, the membranes were blocked in 5% non-fat milk for 1 h at room temperature and incubated with primary antibodies overnight at 4 °C. The membranes were then washed and incubated with secondary antibodies for 2 h at room temperature and developed using ECL detection. Signals were detected with Tanon-5200 Chemiluminescent Imaging System (Tanon, Shanghai, China). The protein levels were analyzed by Image J (NIH, Bethesda, USA) and normalized to the corresponding GAPDH level.

### Quantitative RT-PCR

Total RNAs were extracted from BV2 cells and primary microglia using TRIzol reagent (Life Technologies, USA) according to the manufacturer's instructions. RNA concentrations were equalized and converted to cDNA using Hiscript II reverse transcriptase kit (Vazyme, Nanjing, China). Gene expression was measured by quantitative PCR system (Roche, Basel, Switzerland) using SYBR-green (Roche, Basel, Switzerland). Gene expression was normalized to GAPDH. The sequences of primers used in the experiments are listed in **Table 1**.

### Plasmid transfection and small interfering RNA knockdown

The coding sequence of mouse HSP90 $\beta$  was cloned into pCMV3-untagged vector to construct pHSP90 $\beta$ . All electroporation experiments were

performed using a Neon system and a Neon transfection kit according to the manufacturer's instructions (Invitrogen, California, USA).

**Table 1.** Nucleotide sequences of gene-specific primers used for quantitative real-time PCR.

Gene name	Sequences of forward and reverse primers (5' to 3')
<i>ABCA1</i>	AAAACCGCAGACATCCTTCAG CATACCGAAACTCGTTCACCC
<i>CD36</i>	AGATGACGTGGCAAAGAACAG CCTTGGCTAGATAACGAACCTCTG
<i>ApoE</i>	CTGACAGGATGCCTAGCCG CGCAGGTAATCCCAGAAGC
<i>SRA</i>	TGAAGACGAGGACATGCCATC GAGGTACAAAATCCGCACCTGA
<i>LXR<math>\alpha</math></i>	CCTTCTCAAGGACTTCAGTTACAA CATGGCTCTGGAGAACTCAAAGAT
<i>LXR<math>\beta</math></i>	AAGGACTTCACCTACAGCAAGGA GAACTCGAAGATGGGATTGATGA
<i>ABCG1</i>	AAGGCTACTACCTGGCAAAGA GCAGTAGGCCACAGGGAACA
<i>GAPDH</i>	AGGTCGGTGTGAACGGATTTC TGTAGACCATGTAGTTGAGGTCA

### Generation of pPPRE-Luc reporter plasmid and luciferase assay

Three peroxisome proliferator response element (PPRE) binding sites (5'-AGGGGACCAGGACAAAGGTCACGTTTCGGGA-3') were inserted into pGL4.26 by primer annealing to generate PPAR $\gamma$  reporter plasmids, pPPRE-Luc (**Figure S1A**). HEK293T cells were transfected with pPPRE-Luc. After 24 h, cells were incubated with DMSO or compounds at different concentrations for 24 h. The luciferase activity was measured with luciferase assay system reagent following the manufacturer's protocol (Promega, Madison, USA).

### Immunofluorescence confocal microscopy

Formaldehyde-fixed cells or frozen sections of brain tissue were blocked with 5% normal donkey serum and incubated with indicated primary antibodies at 4 °C overnight, and then incubated with FITC-labeled secondary antibodies (Jackson, USA) for 1 h at room temperature. DAPI (Thermo, USA) was added and incubated with cells or tissue sections for 15 min and mounted with Fluoromount (KeyGen, Nanjing, China). Immunofluorescence was visualized and captured on a confocal microscope (LSM 710, Zeiss, Germany).

### Statistical analysis

All data were expressed as mean  $\pm$  SD. Comparisons between two groups were assessed using Student's *t*-test, and comparisons between three or more sets of data were made using one-way or two-way ANOVA followed by Dunnett's *post hoc* test. Differences with *p* < 0.05 were considered to be statistically significant.

## Results

### A $\beta$ induces the depletion of HSP90 and PPAR $\gamma$

Excess misfolded and damaged proteins overwhelm cellular chaperones, and thus cause functional impairment [39, 40]. We first investigated whether the accumulation of A $\beta$  affects HSP90 and PPAR $\gamma$ . Brain tissues from 8-month-old APP/PS1 mice were collected and subjected to western blot analyses. Results showed that protein levels of HSP90 and PPAR $\gamma$  were reduced (**Figure 1A**). We then checked whether A $\beta$  affects HSP90 and PPAR $\gamma$  in microglia. BV2 cells or primary microglia were treated with A $\beta$ 42 (5  $\mu$ M). After exposure to A $\beta$ 42, the levels of HSP90 in BV2 cells (**Figure 1B**) or primary microglia (**Figure 1C**) were slightly increased at 6 h, and then decreased over time. PPAR $\gamma$  levels exhibited a time-dependent decrease. We then used co-IP to investigate the interaction between PPAR $\gamma$  and HSP90. We observed that there was a loss of interaction between PPAR $\gamma$  and HSP90 after A $\beta$ 42 administration in both BV2 (**Figure 1D**) and primary microglia (**Figure 1E**). Altogether, these results demonstrated that A $\beta$ 42 not only decreased HSP90 and PPAR $\gamma$  protein levels, but also disrupted the binding between HSP90 and PPAR $\gamma$ .

HSP90 has three family members: the constitutive and ubiquitous isoform HSP90 $\beta$ , the stress-inducible and tissue-specific isoform HSP90 $\alpha$ , and the mitochondrial form of TRAP. Human HSP90 $\alpha$  shows 85.8% amino acid sequence identity to HSP90 $\beta$  [41]. Interestingly, in BV2 cells, A $\beta$ 42 (5  $\mu$ M) incubation for 6 h and 12 h led to a decrease of HSP90 $\beta$  and PPAR $\gamma$ , but did not change the levels of HSP90 $\alpha$  (**Figure 1F**). To further identify which paralog of HSP90 is involved in the A $\beta$ 42-induced decrease of PPAR $\gamma$ , we separately knocked down HSP90 $\alpha$  or HSP90 $\beta$  in BV2 cells using siRNA. Transfection of BV2 cells with siRNA effectively decreased HSP90 $\alpha$  or HSP90 $\beta$  expression, respectively (**Figure 1G**). It was noted that knockdown of HSP90 $\beta$ , instead of HSP90 $\alpha$ , significantly decreased PPAR $\gamma$  (**Figure 1G**). Moreover, overexpression of HSP90 $\beta$  in BV2 cells not only increased the basal levels of PPAR $\gamma$ , but also rescued A $\beta$ 42-induced PPAR $\gamma$  decrease (**Figure 1H**). Taken together, the above findings suggest that HSP90 $\beta$ , rather than HSP90 $\alpha$ , is essential for PPAR $\gamma$  stability in microglia.

### JuA activates PPAR $\gamma$ and facilitates A $\beta$ 42 degradation in microglia

Using a stable cell line carrying a luciferase reporter driven by a PPRE-containing promoter (**Figure S1A**), we screened an in-house small

compound pool containing about 350 natural products [42]. JuA (Figure 2A) was found to significantly increase the PPRE-luciferase activity (Figure 2B) and showed negligible cytotoxicity in BV2 cells (Figure S1B) or primary microglia (Figure S1C). The protein level and subcellular localization of PPAR $\gamma$  in BV2 cells were determined by immunofluorescence staining. As shown in Figure 2C, PPAR $\gamma$  was mainly localized in the nuclei. PPAR $\gamma$  was down-regulated after A $\beta$ 42 treatment, while JuA

dose-dependently reversed the A $\beta$ 42 effects on PPAR $\gamma$ . We then examined the expression of PPAR $\gamma$  target genes in BV2 or primary microglia. The expression levels of *CD36*, *SRA3*, *LXR $\alpha$*  and *LXR $\beta$*  were up-regulated after treatment with JuA in a dose-dependent manner. JuA treatment also increased the expression levels of *ApoE*, *ABCG1* and *ABCA1* in BV2 or primary microglia partially *via* the induction of *LXR* expression [9, 43, 44] (Figure 2D-E).

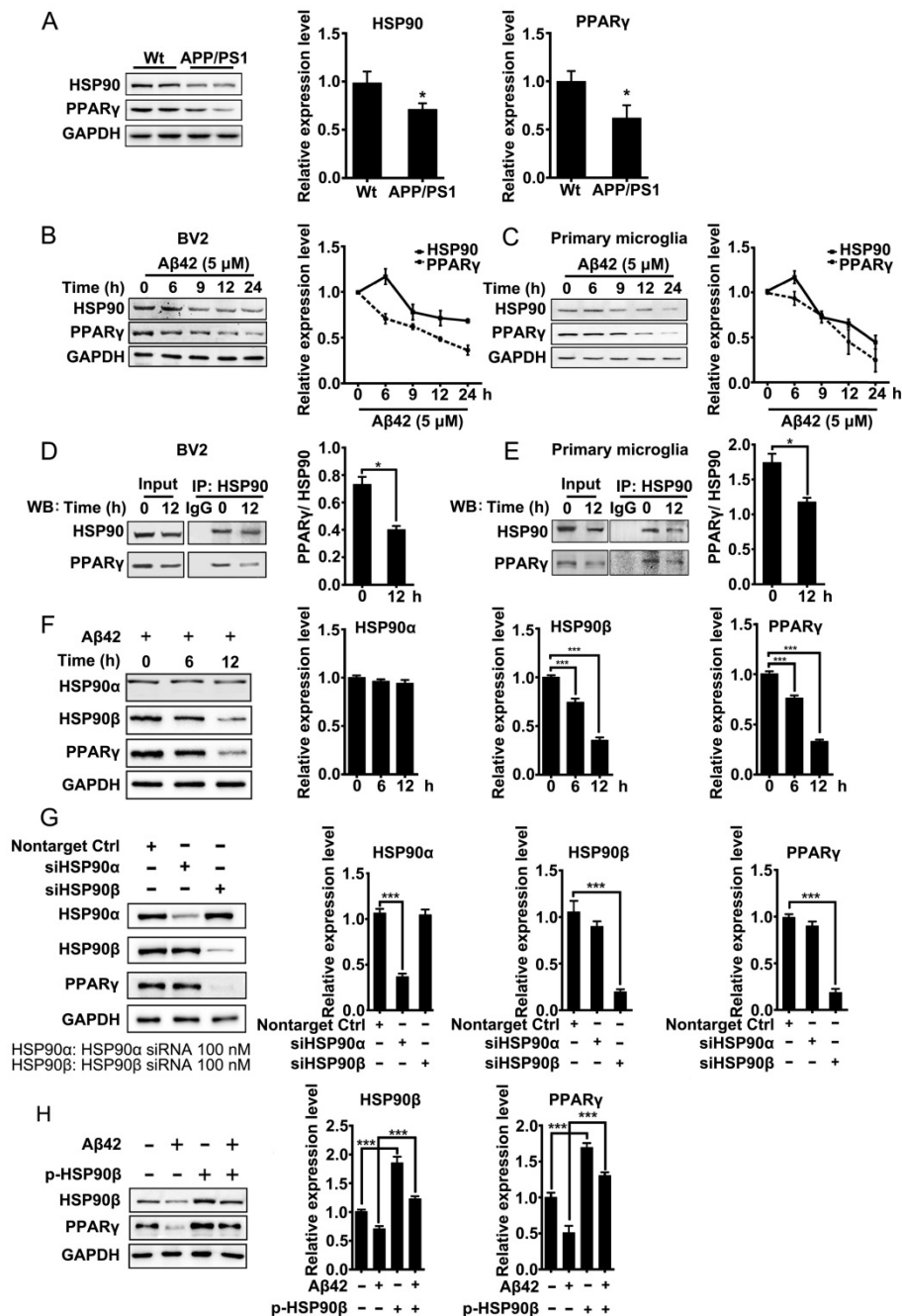


**Figure 1. A $\beta$  induces depletion of HSP90 and PPAR $\gamma$ .** (A) Brain tissue from 8-month-old Wt or APP/PS1 transgenic mice was collected and subjected to Western blot analyses. BV2 cells (B) or primary microglia (C) were administrated A $\beta$ 42 (5  $\mu$ M) for the indicated times. The detergent-soluble lysates from cells were extracted for Western blot assay. BV2 cells (D) or primary microglia (E) were administrated A $\beta$ 42 (5  $\mu$ M) for 12 h. Total protein was extracted and subjected to IP study with indicated antibodies. (F) BV2 cells were incubated with A $\beta$ 42 (5  $\mu$ M) for the indicated times and protein levels of HSP90 $\alpha$ , HSP90 $\beta$  and PPAR $\gamma$  were detected. (G) BV2 cells were transfected with indicated siRNA for 48 h. (H) BV2 cells were transfected with p-HSP90 $\beta$  and administrated A $\beta$ 42 (5  $\mu$ M) for 12 h. Whole cell proteins were collected for western blot assay. All Experiments were repeated three times. \* $p$  < 0.05, \*\*\* $p$  < 0.001 vs. indicated control.

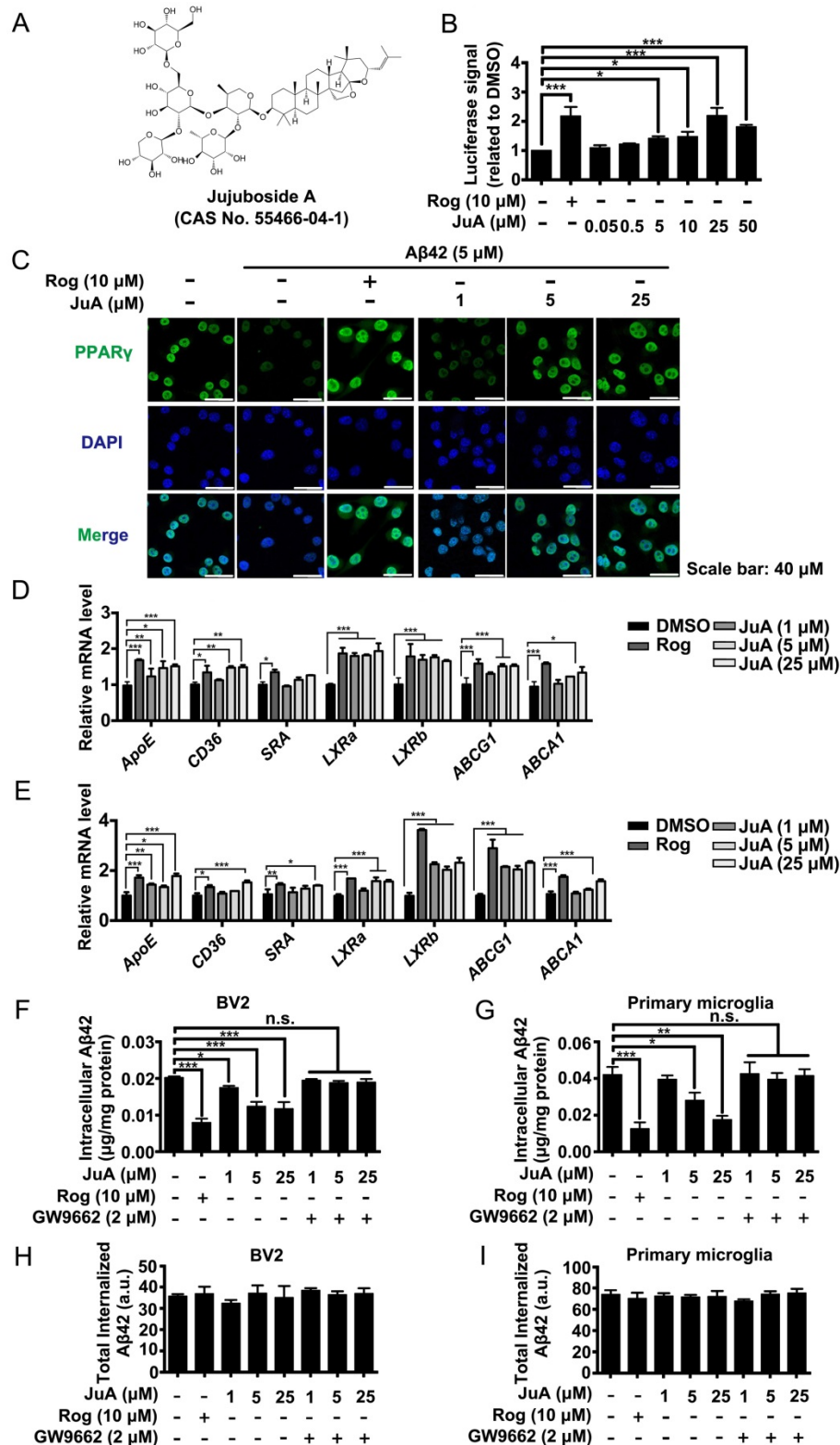


**Figure 2. Aβ induces impaired PPARγ activity in microglia. (A)** The structure and CAS number of JuA. **(B)** HEK293/PPRE-Luc cells were treated with Rog (10 μM) or indicated concentrations of JuA for 24 h, then cells were lysed and luciferase activity was measured. **(C)** BV2 cells were pretreated with JuA for 30 min, followed by administration of Aβ42 (5 μM) for 12 h. Cells were fixed and immunostained with PPARγ antibody. The representative images demonstrate the amount and localization of PPARγ (green). Nuclei were counterstained with DAPI (blue). Scale bar: 40 μm. BV2 cells **(D)** and primary microglia **(E)** were pretreated with JuA for 30 min, followed by administration of Aβ42 (5 μM) for 6 h. The expression of various genes was analyzed by Q-PCR. DMSO at 0.1% was used as control. BV2 cells **(F)** and primary microglia **(G)** were pretreated with JuA at indicated concentrations with or without GW9662 (2 μM) for 18 h, and then incubated with 2 mg/mL Aβ42 in the presence of vehicle (DMSO) or drug for an additional 24 h. The intracellular Aβ42 levels were measured using ELISA. Uptake of Aβ42 by BV2 **(H)** and primary microglia **(I)** was assessed by applying FITC-labeled Aβ42 to microglia after pretreatment with indicated compounds. The accumulation of the fluorophore was analyzed by flow cytometry. The results were normalized to total cellular protein. DMSO at 0.1% was used as control. All experiments were repeated three times. \**p* < 0.05, \*\**p* < 0.01, \*\*\**p* < 0.001 vs. indicated control.

We then investigated whether JuA could promote A $\beta$  degradation in microglia. The intracellular A $\beta$ 42 levels were significantly reduced by JuA treatment both in BV2 (**Figure 2F**) and primary microglia (**Figure 2G**). The A $\beta$ 42 clearance ability of JuA was blocked by GW9662, a specific PPAR $\gamma$  antagonist (**Figure 2F-G**). To exclude the possibility that the reduced A $\beta$ 42 was due to reduced uptake, the cumulative internalization of A $\beta$ 42 was monitored using flow cytometry with FITC-labeled A $\beta$ 42. FITC-labeled A $\beta$ 42 is taken up by microglia and degraded. After A $\beta$ 42 is degraded by microglia, the fluorophore is still retained within the cells, thus the total cellular fluorescence is an independent indicator of total A $\beta$ 42 uptake [45]. As shown in **Figure 2H-I**, the total internalized A $\beta$ 42 levels in BV2 or primary microglia were not affected by drug treatment. Taken together, these data suggest that JuA facilitates the degradation of A $\beta$ 42 in microglia through enhancing PPAR $\gamma$  activity.

### JuA up-regulates PPAR $\gamma$ levels through HSP90 $\beta$

We then checked whether JuA preserved PPAR $\gamma$  in an HSP90 $\beta$ -dependent manner. BV2 cells were

incubated with A $\beta$ 42 (5  $\mu$ M) for 12 h with or without pretreatment with JuA. JuA pretreatment reversed A $\beta$ 42-induced HSP90 $\beta$  and PPAR $\gamma$  decrease in a dose-dependent manner (**Figure 3A**). After BV2 cells were incubated with A $\beta$ 42 (5  $\mu$ M) for 12 h, the interaction between HSP90 $\beta$  and PPAR $\gamma$  was significantly disrupted (**Figure 3B**). JuA (25  $\mu$ M) treatment clearly protected the interaction between HSP90 $\beta$  and PPAR $\gamma$  in a dose-dependent manner. When HSP90 $\beta$  was knocked down in BV2 cells, the activity of JuA was completely reversed (**Figure 3C**). Together, these results indicate that JuA restores protein levels of PPAR $\gamma$  under A $\beta$ 42 stress through increasing HSP90 $\beta$ .

### JuA up-regulates HSP90 $\beta$ in an Axl-dependent manner

It has been reported that the expression of HSP90 $\beta$  could be regulated by ERK [46, 47]. We then tested whether JuA could affect ERK activity. As was shown, JuA increased phosphorylation of ERK in time-dependent (**Figure 4A**) and dose-dependent (**Figure 4B**) manners in BV2 cells. Effects of JuA on HSP90 $\beta$ , as well as PPAR $\gamma$ , were blocked by SCH772984, an ERK-specific inhibitor (**Figure 4C**).

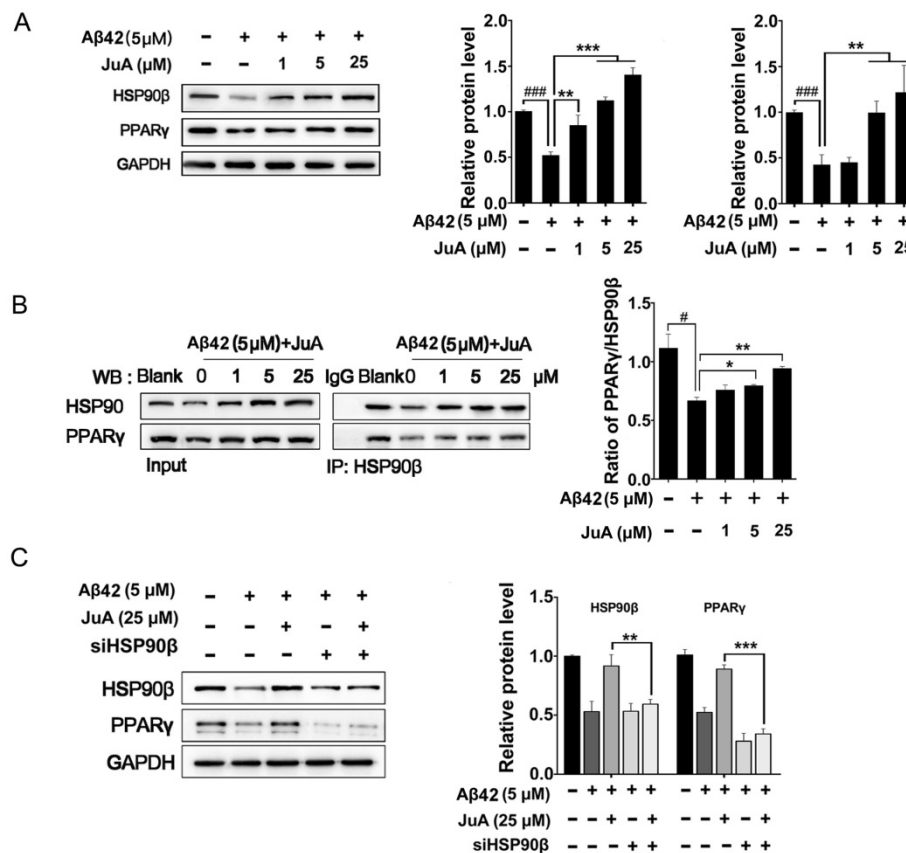


**Figure 3. HSP90 $\beta$  is essential for maintaining PPAR $\gamma$  function in microglia.** BV2 cells were pretreated with JuA at 1  $\mu$ M, 5  $\mu$ M or 25  $\mu$ M for 30 min, followed by administration of A $\beta$ 42 (5  $\mu$ M) for 12 h. Total protein was extracted and subjected to western blot (**A**) and IP study (**B**) with indicated antibodies. (**C**) BV2 cells were transfected with HSP90 $\beta$  siRNA for 48 h, and then pretreated with JuA for 30 min followed by administration of A $\beta$ 42 (5  $\mu$ M) for 12 h. DMSO at 0.1% was used as Ctrl. Whole cell proteins were collected for western blot assay. All experiments were repeated three times. ### $p$  < 0.001, \* $p$  < 0.05, \*\* $p$  < 0.01, \*\*\* $p$  < 0.001.

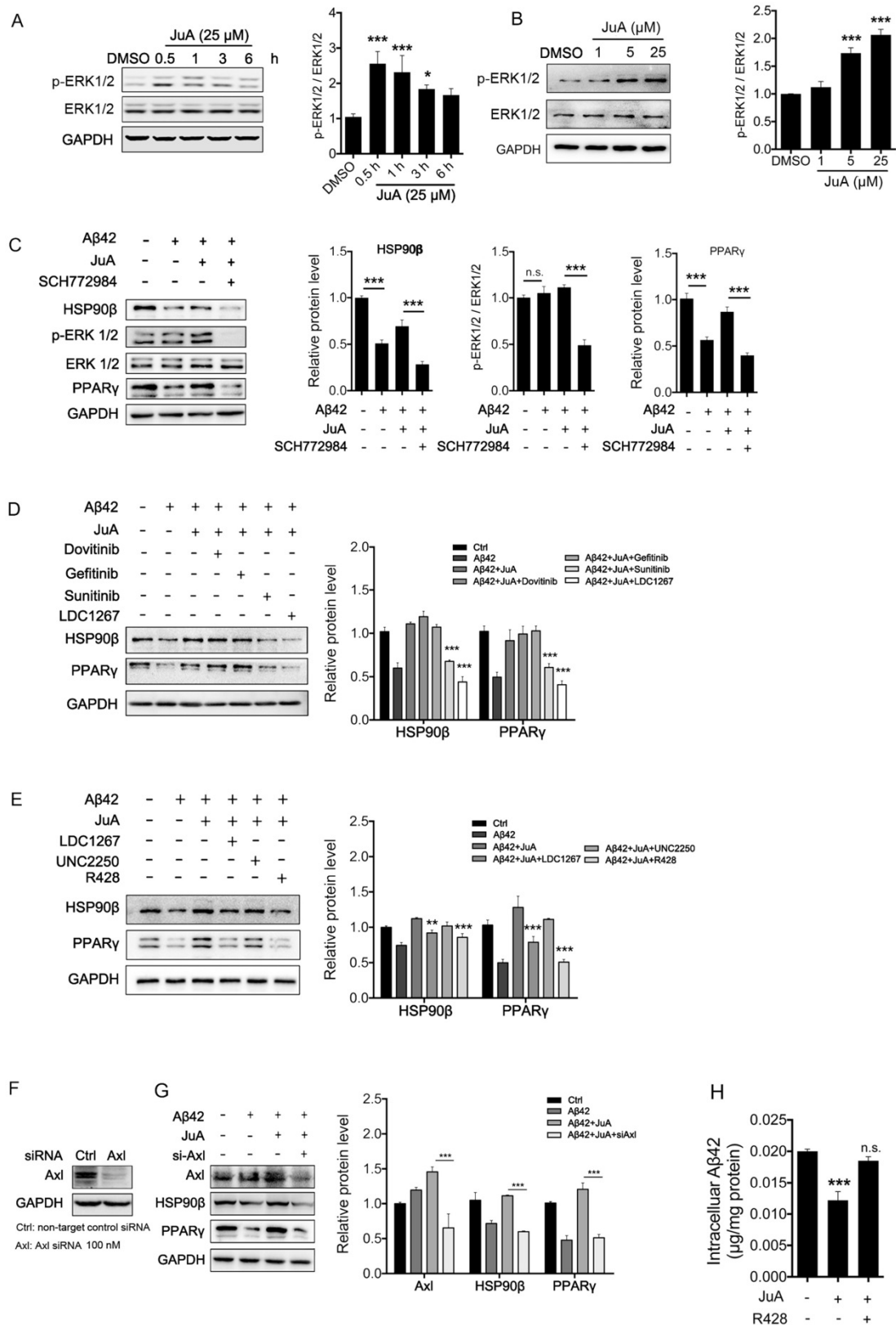


**Figure 4. JuA up-regulates HSP90β in an Axl/ERK-dependent manner.** BV2 cells were treated with JuA (25 μM) for indicated periods of time (A), or treated with JuA at indicated concentrations for 0.5 h (B). (C) BV2 cells were pretreated with 0.1% DMSO (Ctrl), JuA (25 μM) or JuA (25 μM) + SCH772984 (10 μM) for 30 min, followed by administration of Aβ42 (5 μM) for 6 h. (D) BV2 cells were pretreated with 0.1% DMSO (Ctrl), JuA (25 μM) or JuA (25 μM) with the indicated antagonist of RTKs (Dovitinib at 1 μM, Gefitinib at 2.5 μM, Sunitinib at 2.5 μM and LDC1267 at 1 μM) for 30 min, followed by administration of Aβ42 (5 μM) for 12 h. (E) BV2 cells were pretreated with 0.1% DMSO (Ctrl), JuA (25 μM) or JuA (25 μM) with the indicated antagonist of TAM receptor (LDC1267 at 1 μM, UNC2250 at 5 μM, R428 at 5 μM) for 30 min, followed by administration of Aβ42 (5 μM) for 12 h. (F) BV2 cells were transiently transfected with non-target control siRNA or siAxl for 48 h. (G) BV2 cells were transfected with siAxl for 48 h, then pretreated with JuA (25 μM) followed by administration of Aβ42 (5 μM) for 12 h. The whole-cell proteins were subjected to western blot with the antibodies indicated. All experiments were repeated three times. \*p < 0.05, \*\*p < 0.01, \*\*\*p < 0.001.

As RTK is one of the most important upstream regulators of ERK [48-50], we next investigated whether RTK is involved in the activation of JuA. We applied a non-specific RTK antagonist (Sunitinib), and specific antagonists targeting the key membrane receptors of microglia, including EGFR (Dovitinib), VEGFR (Gefitinib) and TAM receptor (LDC1267), to identify which subtype of RTKs is essential for JuA activity. As shown in **Figure 4D**, pretreatment with Sunitinib and LDC1267 completely reversed JuA-induced up-regulation of HSP90 $\beta$ , strongly indicating that TAM receptors are involved in the JuA activity. Axl and Mer are the main types of TAM receptors that are expressed in microglia [51]; we further treated BV2 cells with JuA in the presence of specific inhibitors targeting Axl (R428) or Mer (UNC2250). It was shown that R428 strongly suppressed JuA-induced HSP90 $\beta$  expression (**Figure 4E**), while UNC2250 did not affect JuA activity. To further confirm the results, we knocked down Axl using siRNAs in BV2 cells (**Figure 4F**), and observed that Axl knockdown completely reversed the effect of JuA on HSP90 $\beta$  and PPAR $\gamma$  (**Figure 4G**). Moreover, R428 could also inhibit JuA-induced A $\beta$ 42 clearance in BV2 cells (**Figure 4H**). Taken together, these results suggest that JuA increases HSP90 $\beta$  expression and preserves PPAR $\gamma$  activity through the Axl/ERK pathway.

### **JuA ameliorates cognitive deficiency in APP/PS1 transgenic mice models and decreases A $\beta$ accumulation in the brain**

To further test the *in vivo* effects of JuA, 8-month-old APP/PS1 transgenic mice were applied, which simulate the late-onset pathological process of AD in humans [52]. At the age of 8 months, APP/PS1 transgenic mice develop abundant plaques in the hippocampus and cortex [53], and show deficits in learning and memory [54].

The animal experimental design is depicted in **Figure 5A**. Mice were treated with vehicle (0.1% DMSO-saline, i.t.), Rog (0.5 mg/kg, i.t.) or JuA (0.5 mg/kg, 1.5 mg/kg or 5 mg/kg, i.t.) once daily for 7 days. The MWM test and object recognition test were performed to evaluate the effect of JuA on APP/PS1 transgenic mice.

In the MWM test, the APP/PS1 group displayed significantly longer escape latency compared to the wild-type littermate control mice (Wt) group during spatial acquisition training, which can be improved by JuA treatment (**Figure 5B**). The swim speed was not altered after treatment (**Figure 5C**). In the spatial probe test, the distance and time in the target quadrant and the platform crossing numbers of the

APP/PS1 group were significantly lower than those of the Wt group, indicating the impairment of spatial memory capacity, which can be reversed by JuA treatment in a dose-dependent manner (**Figure 5D-G**).

The procedure used for the object recognition test is shown in **Figure 5H**. In the object recognition test, the discrimination index was used to evaluate learning and memory ability in mice, where a higher index value indicates greater preference for the new object. The Wt mice group preferred the novel objects while the APP/PS1 group showed no significant preference. Administration of JuA at doses of 1.5 mg/kg and 5 mg/kg effectively cured the impaired learning and memory ability of APP/PS1 transgenic mice and the discrimination values were significantly higher than those of the APP/PS1 group (**Figure 5I-J**). Moreover, the A $\beta$ 42 levels in the cortex (**Figure 5K**) and hippocampus (**Figure 5L**) were down-regulated by JuA treatment. Similar results were observed when JuA was administrated orally (**Figure S2**). These results demonstrate that JuA ameliorates cognitive deficiency and reduces A $\beta$ 42 accumulation in the brains of APP/PS1 transgenic mice.

### **JuA ameliorates the cognitive deficiency in APP/PS1 mice through Axl**

The effect of JuA in APP/PS1 mice could be blocked by the PPAR $\gamma$ -specific inhibitor GW9662 (**Figure S3**); these results agree with the *in vitro* study. We then validated whether JuA promotes A $\beta$ 42 clearance *via* Axl *in vivo*. The APP/PS1 transgenic mice were administrated JuA (5 mg/kg, i.t.) alone or treated with JuA and R428 (3.5 mg/kg, i.t., 30 min before the JuA administration), once daily for 7 days. In the MWM test, the JuA-treated group showed significantly shorter escape latency in spatial acquisition training compared to the APP/PS1 group. However, pretreatment with Axl inhibitor R428 abolished the effect of JuA (**Figure 6A**). In the spatial probe test, the distance and time spent in the target quadrant, and platform crossing numbers were increased by JuA treatment, while R428 reversed the effect of JuA (**Figure 6B-E**). Similarly, in the object recognition test, the discrimination index cured by JuA was also reversed by R428 (**Figure 6F-G**). These results suggest that Axl is essential for the memory recovery effects of JuA in APP/PS1 mice.

In addition, A $\beta$ 42 levels in the cortex and hippocampus were both down-regulated by JuA, which was completely blocked by R428 (**Figure 6H-I**). Taken together, these results indicate that JuA ameliorates cognitive deficiency and decreases the accumulation of A $\beta$ 42 in an Axl-dependent manner.

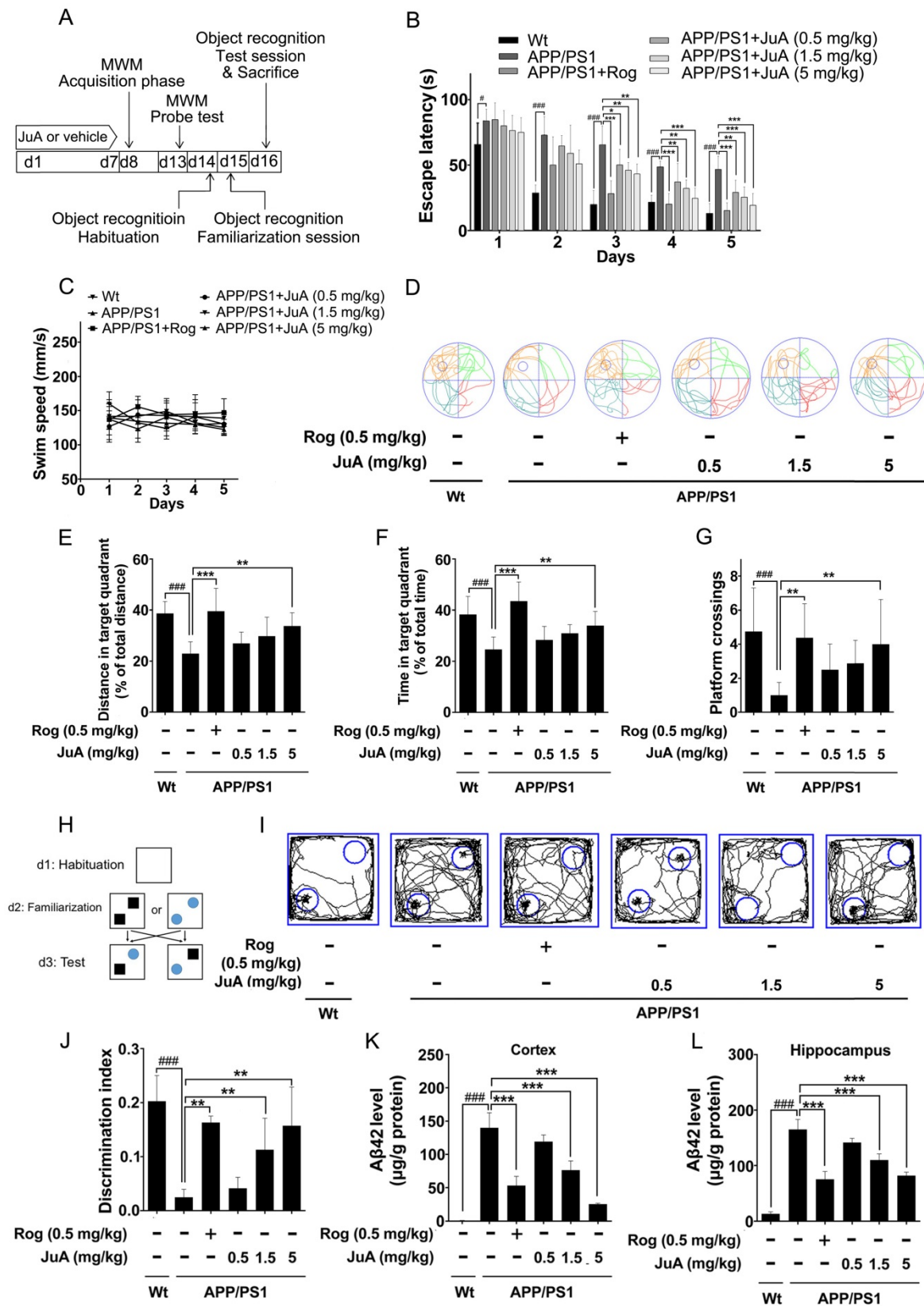


**Figure 5. JuA ameliorates the cognitive deficiency in APP/PS1 mice. (A)** Experimental design for the animal study. 8-mon-old APP/PS1 mice were treated with saline (i.t.), Rog (0.5 mg/kg, i.t.) or JuA (0.5 mg/kg, 1.5 mg/kg, 5 mg/kg, i.t.) once daily for 7 days. **(B)** Escape latency and **(C)** swim speed during spatial acquisition training. **(D)** Representative motion track, **(E)** distance in the target quadrant, **(F)** time spent in the target quadrant and **(G)** the platform crossing number in the spatial probe test. **(H)** The procedure for the object recognition test. **(I)** Representative motion track and **(J)** the discrimination index in the object recognition test. After the MWM test and the object recognition test, animals were sacrificed and the brain tissues were collected. Aβ42 levels in the cortex **(K)** and hippocampus **(L)** were detected by ELISA. #  $p < 0.05$ , ###  $p < 0.001$  vs. Wt group. \*  $p < 0.05$ , \*\*  $p < 0.01$ , \*\*\*  $p < 0.001$  vs. APP/PS1 group.

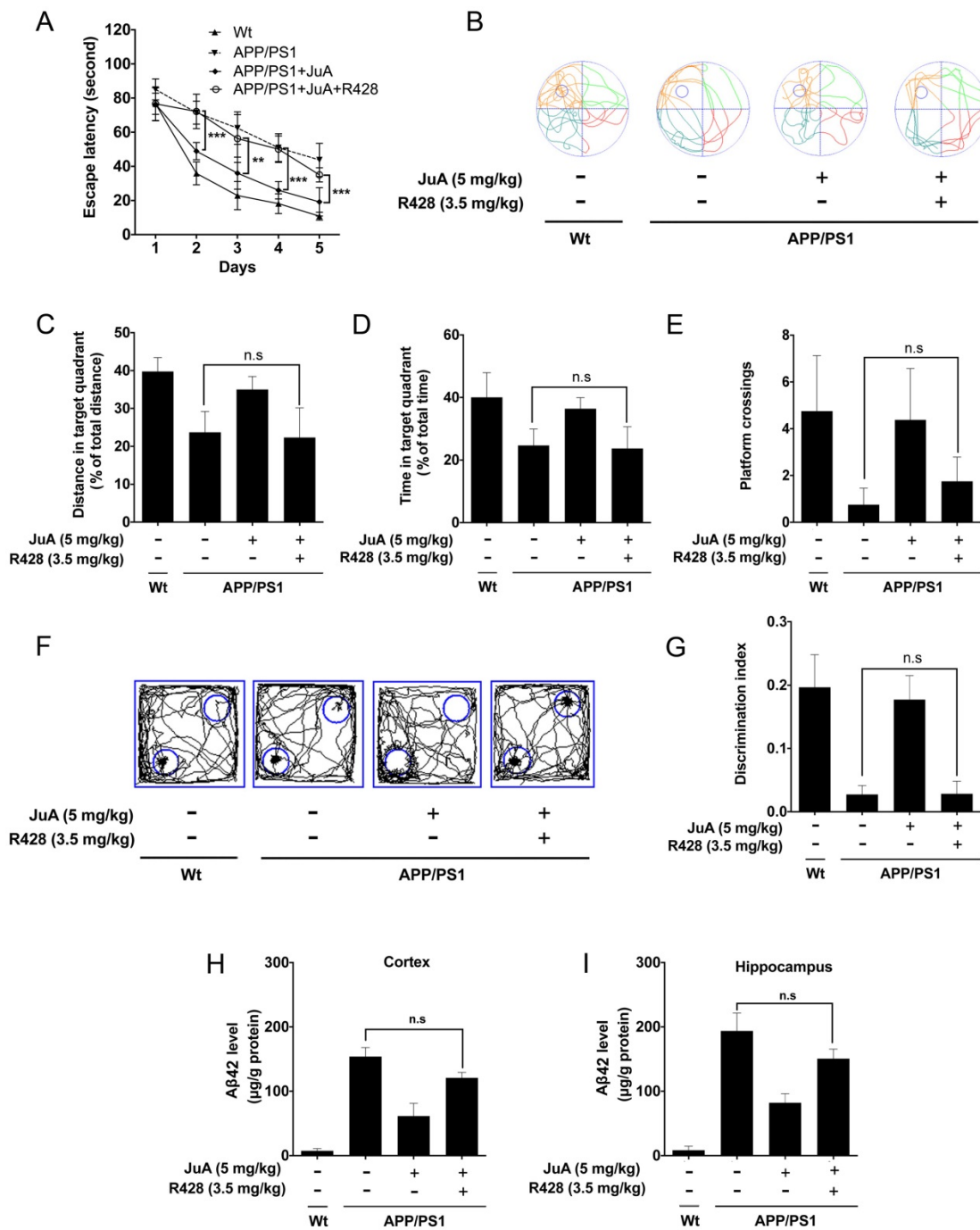


**Figure 6. JuA ameliorates the cognitive deficiency in APP/PS1 mice through Axl.** 8-month-old APP/PS1 mice were treated with JuA (5 mg/kg, i.t.) or treated with JuA and R428 (3.5 mg/kg, i.t.) once daily for 7 days. **(A)** Escape latency during spatial acquisition training, **(B)** Representative motion track, **(C)** distance in the target quadrant, **(D)** time spent in the target quadrant, and **(E)** the platform crossing number in the spatial probe test. **(F)** Representative motion track and **(G)** discrimination index in the object recognition test. **(H)** After the MWM test and the object recognition test, animals were sacrificed and the brain tissues were collected. Aβ42 levels in the cortex and hippocampus were detected by ELISA. \*  $p < 0.01$ , \*\*\*  $p < 0.001$ .

### JuA reduces plaques and relieves over-activation of microglia in the brain

The above results showed that JuA treatment decreased the levels of soluble Aβ. We then validated whether JuA promotes the clearance of insoluble plaques. Wide distribution of thioflavin-S<sup>+</sup> plaques (indicative of insoluble plaques) in the cortex and hippocampus were observed in the brains of

APP/PS1 transgenic mice. JuA treatment significantly reduced the insoluble plaques number both in the cortex and hippocampus. R428 blocked the effect of JuA (Figure 7A), indicating Axl plays a pivotal role in the function of JuA for the clearance of Aβ42.

The abnormal accumulation of Aβ induces excessive activation of microglia in the brain, which is associated with neuron injury in AD [55]. Iba-1 is a calcium-binding protein that is specifically expressed

in brain microglia and up-regulated upon microglia activation [56]. We then detected Iba-1-positive cells in the brain by immunofluorescence staining, and quantified Iba-1 level in the cortex and hippocampus by western blot. As shown in **Figure 7B**, cells with precise Iba-1-positive staining of the cytoplasm were identified as microglia in the brain tissues. Strong activation of microglia was found in the brains of APP/PS1 mice. JuA treatment significantly inhibited the activation of microglia, while the effects of JuA on

microglia were greatly inhibited by R428. Western blot results showed that Iba-1 levels were elevated in the cortex and hippocampus of APP/PS1 mice (**Figure 7C**). JuA treatment significantly decreased Iba-1 expression in brain tissues of APP/PS1 mice, which was reversed by R428 (**Figure 7C**). The above data suggest that JuA promotes the clearance of both soluble and insoluble A $\beta$  plaques, and inhibits abnormal activation of microglia *in vivo* in an Axl-dependent manner.

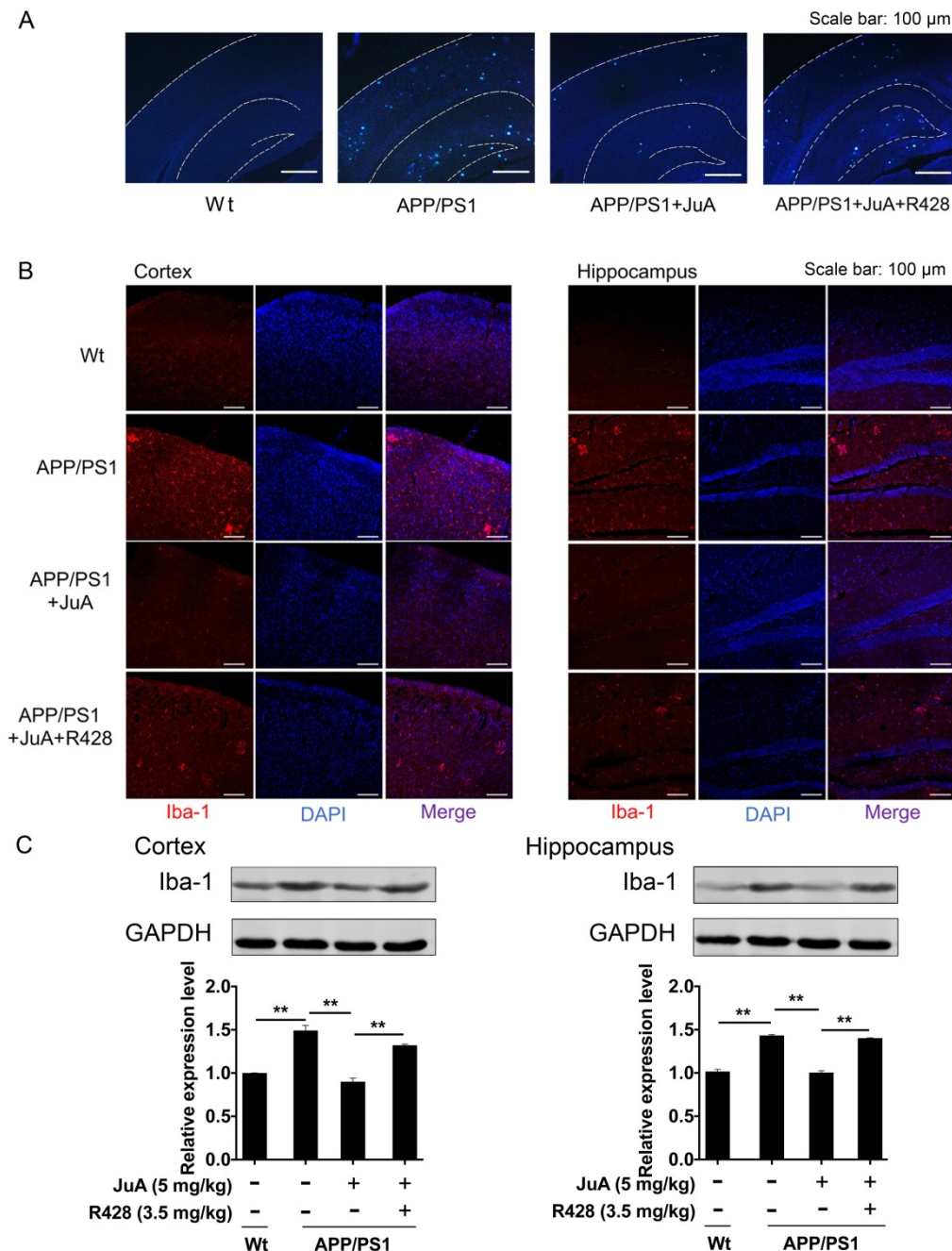


**Figure 7. JuA reduces plaques and relieves over-activation of microglia in the brain.** 8-month-old APP/PS1 mice were treated with JuA (5 mg/kg, i.t.) or treated with JuA and R428 (3.5 mg/kg, i.t., 30 min before the JuA administration) once daily for 7 days. **(A)** Representative cortex and hippocampus sections stained with thioflavin S. Scale bar: 100  $\mu$ m. **(B)** Brain tissues were fixed and stained with Iba-1 primary antibody, then imaged by immunofluorescence confocal microscopy (red). Nuclei were stained with DAPI (blue). Representative image demonstrating the morphology of microglia in the cortex and hippocampus. Scale bar: 100  $\mu$ m. **(C)** Iba-1 levels in the cortex and hippocampus detected by Western blot. \*\*  $p < 0.01$

## Discussion

The integrity of the proteome is challenged with age and progression of AD pathology. Chaperones have an important role in the repair of proteotoxic damage [39]. The content of chaperones, such as HSP90, decreases during ageing due to the increased amount of damaged proteins [21, 57]. In recent years, especially heat shock proteins (HSPs) chaperones have been considered as critical regulators of proteins-associated neurodegenerative diseases [58]. Cytosolic HSP70 and HSP90 inhibit early stages of amyloid aggregation [59]. Carboxy-terminus of Hsc70-interacting protein (CHIP) has also been found to be critical for tau degradation and this association is facilitated by HSP70 [60]. HSP90 was found to enhance the phagocytosis and degradation of A $\beta$ 42 by microglia both *in vitro* and *in vivo* [61, 62]. Since the accumulation of A $\beta$  in the brain is considered the primary factor in driving AD pathogenesis, we wondered whether A $\beta$  accumulation could also affect the ability of chaperones in microglia, which are responsible for A $\beta$  homeostasis. Our results showed that protein levels of HSP90 were decreased in microglia incubated with A $\beta$ 42 peptides (**Figure 1**). Further study indicated that the levels of HSP90 $\alpha$  did not alter in the presence of A $\beta$ 42, suggesting that, although highly conserved, these different family members play different roles in stressed conditions. Therefore, a HSP90 $\beta$ -specific activator might provide satisfactory therapeutic effects for AD.

It has been reported that HSP90 $\beta$  plays a critical role in PPAR $\gamma$  stability and cellular differentiation in adipocytes [26], human hepatoma cells and mouse livers [63]. Similarly, here we demonstrated that the stability and functions of PPAR $\gamma$  in microglia could be regulated by HSP90 $\beta$ . A $\beta$  stress or knockdown of HSP90 $\beta$  dampened PPAR $\gamma$  in microglia (**Figure 1**). In this study, we found that JuA increased the expression of HSP90 $\beta$ , and enhanced the interaction between HSP90 $\beta$  and PPAR $\gamma$  (**Figure 2**). As knockdown of HSP90 $\beta$  reversed the effects of JuA, we conclude that HSP90 $\beta$  is a major downstream effector of JuA (**Figure 3**).

It has been showed that the MEK/ERK pathway regulates the expression of HSP90 $\beta$  [47]. Axl, one of the upstream regulators of ERK, was found to regulate ERK pathway in different cells including chondrocytes [64], cardiac fibroblasts [65] and several tumor cells [66]. Axl is a member of TAM receptors, which belong to RTKs [67]. In the CNS, Tyro3 is abundant in neurons [68], whereas Mer and Axl are present in microglia [69-71]. Axl functions as controller of microglial physiology [51]. Up-regulation of Axl in microglia licenses their phagocytic activity and promotes plaque clearance

[72]. Our results suggested that the mechanism of HSP90 $\beta$  up-regulation by JuA in BV2 cells is, at least partially, through an Axl/ERK-dependent manner, since the effect of JuA on HSP90 $\beta$  can be blocked by ERK inhibitor SCH772984, Axl antagonist R428, as well as Axl siRNA (**Figure 4**). Moreover, the *in vivo* effects of JuA were also inhibited by R428. It is interesting that the expression of Axl is also regulated by the nuclear receptors (NRs) pathway. Retinoid X receptor (RXR) forms obligate heterodimers with PPAR $\gamma$  and comprise the functional transcription factor [73]. Savage et al. has reported that bexarotene, an agonist of RXR, increases Mer and Axl expression in plaque-associated immune cells, consequently licensing their phagocytic activity and promoting plaque clearance [72]. Combined with our findings, the above results suggest a positive feedback between Axl and PPAR $\gamma$  signaling pathway, which may explain the notable high-efficiency clearing of both soluble A $\beta$  and insoluble plaques in the brain after treatment with JuA (**Figure 6** and **Figure 7**).

In the present study, we mainly focused on the process of microglia since they function as phagocytes in the brain and are responsible for A $\beta$  clearance [11]. Astrocytes mediate the degradation of extracellular A $\beta$  through secrete proteases [74]. Several reports have shown that astrocytes also have the ability to take up A $\beta$  [75, 76]. A recent study found that activated PPAR $\gamma$  in astrocytes increases the expression of lipidated ApoE and might participate in clearance of insoluble A $\beta$  [9]. Therefore, the clearance of deposited plaques in APP/PS1 mice by JuA could also be partially attributed to astrocytes activation.

In conclusion, the present study showed that the levels and functions of PPAR $\gamma$  were impaired under A $\beta$  stress due to the decrease of HSP90 $\beta$  in microglia. The small molecule JuA increased the expression of HSP90 $\beta$  and maintained the stability of PPAR $\gamma$  in an Axl/ERK-dependent manner, and enhanced A $\beta$  clearance in microglia (**Figure 8**). Interestingly, our study also showed that JuA inhibited A $\beta$  or DL-homocysteine-induced tau protein phosphorylation (**Figure S4**). JuA treatment effectively ameliorated learning and memory deficiencies in APP/PS1 transgenic mice. Our study sheds some light on the key role of HSP90 $\beta$  in microglia function, and indicates that JuA can serve as a leading compound for the pharmacological control of AD.

## Abbreviations

A $\beta$ : amyloid  $\beta$ ; CNS: central nervous system; ELISA: enzyme-linked immunosorbent assay; FBS: fetal bovine serum; Hcy: DL-homocysteine; HSP90: heat shock protein 90; i.t.: intrathecal; JuA: jujuboside A; MWM: morris water maze; PPAR $\gamma$ : peroxisome

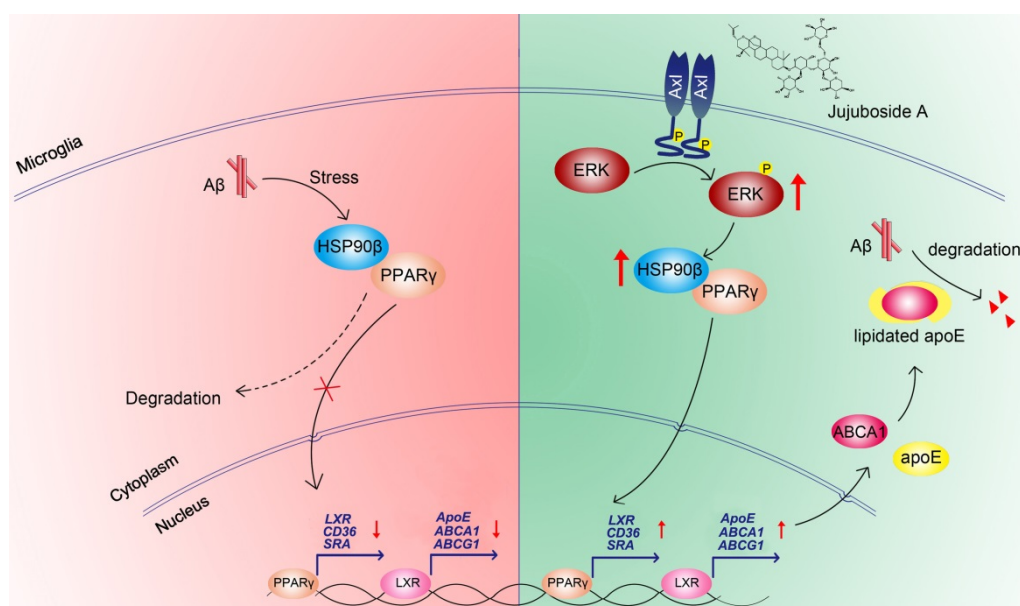


**Figure 8.** Proposed mechanism of JuA-mediated A $\beta$  clearance.

proliferator activated receptor  $\gamma$ ; PPRE: peroxisome proliferator response element; Rog: rosiglitazone; RXR: retinoid X receptor.

## Supplementary Material

Supplementary figures.

<http://www.thno.org/v08p4262s1.pdf>

## Acknowledgements

This work was supported by National Natural Science Foundation of China (No. 81573637, 81421005), "Twelfth-Five Years" Supporting Programs from the Ministry of Science and Technology of China (No. 2015ZX09101043), the Priority Academic Program Development of Jiangsu Higher Education Institutions (PAPD) and 111 Project (no. B16046).

The authors acknowledge technical support from Ms. Ping Zhou, and Dr. Wenling Dai for animal studies. We thank Mr. David Anderson from Southeast University for English proof reading.

## Competing Interests

The authors have declared that no competing interest exists.

## References

- Blennow K, de Leon MJ, Zetterberg H. Alzheimer's disease. *Lancet*. 2006; 368: 387-403.
- Masters CL, Simms G, Weinman NA, Multhaup G, McDonald BL, Beyreuther K. Amyloid plaque core protein in Alzheimer disease and Down syndrome. *Proc Natl Acad Sci U S A*. 1985; 82: 4245-9.
- Holtzman DM, Morris JC, Goate AM. Alzheimer's disease: the challenge of the second century. *Sci Transl Med*. 2011; 3: 77sr1.
- Hardy J, Selkoe DJ. The amyloid hypothesis of Alzheimer's disease: progress and problems on the road to therapeutics. *Science*. 2002; 297: 353-6.
- Polanco JC, Li C, Bodea LG, Martinez-Marmol R, Meunier FA, Gotz J. Amyloid-beta and tau complexity - towards improved biomarkers and targeted therapies. *Nat Rev Neurol*. 2018; 14: 22-39.
- Sperling RA, Aisen PS, Beckett LA, Bennett DA, Craft S, Fagan AM, et al. Toward defining the preclinical stages of Alzheimer's disease: recommendations from the National Institute on Aging-Alzheimer's Association workgroups on diagnostic guidelines for Alzheimer's disease. *Alzheimers Dement*. 2011; 7: 280-92.
- Mawuenyega KG, Sigurdson W, Ovod V, Munsell L, Kasten T, Morris JC, et al. Decreased clearance of CNS beta-amyloid in Alzheimer's disease. *Science*. 2010; 330: 1774.
- Norden DM, Godbout JP. Microglia of the Aged Brain: Primed to be Activated and Resistant to Regulation. *Neuropathol Appl Neurobiol*. 2013; 39: 19-34.
- Mandrekar-Colucci S, Karlo JC, Landreth GE. Mechanisms underlying the rapid peroxisome proliferator-activated receptor-gamma-mediated amyloid clearance and reversal of cognitive deficits in a murine model of Alzheimer's disease. *J Neurosci*. 2012; 32: 10117-28.
- Mandrekar S, Jiang Q, Lee CY, Koenigsnecht-Talboo J, Holtzman DM, Landreth GE. Microglia mediate the clearance of soluble Abeta through fluid phase macropinocytosis. *J Neurosci*. 2009; 29: 4252-62.
- Rogers J, Strohmeier R, Kovelowski CJ, Li R. Microglia and inflammatory mechanisms in the clearance of amyloid beta peptide. *Glia*. 2002; 40: 260-9.
- Cramer PE, Cirrito JR, Wesson DW, Lee CY, Karlo JC, Zinn AE, et al. ApoE-directed therapeutics rapidly clear beta-amyloid and reverse deficits in AD mouse models. *Science*. 2012; 335: 1503-6.
- Perry VH, Holmes C. Microglial priming in neurodegenerative disease. *Nat Rev Neurol*. 2014; 10: 217.
- Hickman SE, Allison EK, El Khoury J. Microglial dysfunction and defective beta-amyloid clearance pathways in aging Alzheimer's disease mice. *J Neurosci*. 2008; 28: 8354-60.
- Johnston H, Boutin H, Allan SM. Assessing the contribution of inflammation in models of Alzheimer's disease. *Biochem Soc Trans*. 2011; 39: 886-90.
- Chen CH, Zhou W, Liu S, Deng Y, Cai F, Tone M, et al. Increased NF-kappaB signalling up-regulates BACE1 expression and its therapeutic potential in Alzheimer's disease. *Int J Neuropsychopharmacol*. 2012; 15: 77-90.
- Landreth G. PPARgamma agonists as new therapeutic agents for the treatment of Alzheimer's disease. *Exp Neurol*. 2006; 199: 245-8.
- Mrak RE, Landreth GE. PPARgamma, neuroinflammation, and disease. *J Neuroinflammation*. 2004; 1: 209-215.
- Jiang Q, Lee CY, Mandrekar S, Wilkinson B, Cramer P, Zelcer N, et al. ApoE promotes the proteolytic degradation of Abeta. *Neuron*. 2008; 58: 681-93.
- Sastre M, Dewachter I, Rossner S, Bogdanovic N, Rosen E, Borghgraef P, et al. Nonsteroidal anti-inflammatory drugs repress beta-secretase gene

- promoter activity by the activation of PPARgamma. *Proc Natl Acad Sci U S A*. 2006; 103: 443-8.
21. Nardai G, Csermely P, Soti C. Chaperone function and chaperone overload in the aged. A preliminary analysis. *Exp Gerontol*. 2002; 37: 1257-62.
  22. Gezen-Ak D, Dursun E, Hanağası H, Bilgiç B, Lohman E, Araz ÖS, et al. BDNF, TNF $\alpha$ , HSP90, CFH, and IL-10 serum levels in patients with early or late onset Alzheimer's disease or mild cognitive impairment. *J Alzheimers Dis*. 2013; 37: 185-95.
  23. Evans CG, Wisen S, Gestwicki JE. Heat shock proteins 70 and 90 inhibit early stages of amyloid  $\beta$ -(1-42) aggregation in vitro. *J Biol Chem*. 2006; 281: 33182-91.
  24. Schirmer C, Lepvrier E, Duchesne L, Decaux O, Thomas D, Delamarche C, et al. Hsp90 directly interacts, in vitro, with amyloid structures and modulates their assembly and disassembly. *Biochim Biophys Acta*. 2016; 1860: 2598-609.
  25. Feder ME, Hofmann GE. Heat-shock proteins, molecular chaperones, and the stress response: evolutionary and ecological physiology. *Annu Rev Physiol*. 1999; 61: 243-82.
  26. Nguyen MT, Csermely P, Soti C. Hsp90 chaperones PPARgamma and regulates differentiation and survival of 3T3-L1 adipocytes. *Cell Death Differ*. 2013; 20: 1654-63.
  27. Han D, Wan C, Liu F, Xu X, Jiang L, Xu J. Jujuboside A Protects H9C2 Cells from Isoproterenol-Induced Injury via Activating PI3K/Akt/mTOR Signaling Pathway. *Evid Based Complement Alternat Med*. 2016; 2016: 9593716.
  28. Liu Z, Zhao X, Liu B, Liu AJ, Li H, Mao X, et al. Jujuboside A, a neuroprotective agent from semen Ziziphi Spinosa ameliorates behavioral disorders of the dementia mouse model induced by Abeta 1-42. *Eur J Pharmacol*. 2014; 738: 206-13.
  29. Wang XX, Ma GL, Xie JB, Pang GC. Influence of JuA in evoking communication changes between the small intestines and brain tissues of rats and the GABAA and GABAB receptor transcription levels of hippocampal neurons. *J Ethnopharmacol*. 2015; 159: 215-23.
  30. Tamashiro TT, Dalgard CL, Byrnes KR. Primary microglia isolation from mixed glial cell cultures of neonatal rat brain tissue. *J Vis Exp*. 2012: e3814.
  31. Stine WB, Jr., Dahlgren KN, Krafft GA, LaDu MJ. In vitro characterization of conditions for amyloid-beta peptide oligomerization and fibrillogenesis. *J Biol Chem*. 2003; 278: 11612-22.
  32. Tobinick EL. Perispinal Delivery of CNS Drugs. *CNS Drugs*. 2016; 30: 469-80.
  33. Shi JQ, Wang BR, Jiang WW, Chen J, Zhu YW, Zhong LL, et al. Cognitive improvement with intrathecal administration of infliximab in a woman with Alzheimer's disease. *J Am Geriatr Soc*. 2011; 59: 1142-4.
  34. Dai WL, Xiong F, Yan B, Cao ZY, Liu WT, Liu JH, et al. Blockade of neuronal dopamine D2 receptor attenuates morphine tolerance in mice spinal cord. *Sci Rep*. 2016; 6: 38746.
  35. Morris R. Developments of a water-maze procedure for studying spatial learning in the rat. *J Neurosci Methods*. 1984; 11: 47-60.
  36. Leger M, Quiedeville A, Bouet V, Haelewyn B, Boulouard M, Schumann-Bard P, et al. Object recognition test in mice. *Nat Protoc*. 2013; 8: 2531-7.
  37. Erica Korb MH, Ilana Zucker-Scharff, Robert B Darnell, C David Allis. BET protein Brd4 activates transcription in neurons and BET inhibitor Jq1 blocks memory in mice. *Nat Neurosci*. 2015; 18: 13.
  38. Rajamaheswari HB, Sigurdsson EM. Histological staining of amyloid and pre-amyloid peptides and proteins in mouse tissue. *Methods Mol Biol*. 2012; 849: 411-24.
  39. Vilchez D, Saez I, Dillin A. The role of protein clearance mechanisms in organismal ageing and age-related diseases. *Nat Commun*. 2014; 5: 5659.
  40. Eisenberg D, Jucker M. The amyloid state of proteins in human diseases. *Cell*. 2012; 148: 1188-203.
  41. Chen B, Piel WH, Gui L, Bruford E, Monteiro A. The HSP90 family of genes in the human genome: insights into their divergence and evolution. *Genomics*. 2005; 86: 627-37.
  42. Wang J, Shi ZQ, Zhang M, Xin GZ, Pang T, Zhou P, et al. Camptothecin and its analogs reduce amyloid-beta production and amyloid-beta42-induced IL-1beta production. *J Alzheimers Dis*. 2015; 43: 465-77.
  43. Li AC, Binder CJ, Gutierrez A, Brown KK, Plotkin CR, Pattison JW, et al. Differential inhibition of macrophage foam-cell formation and atherosclerosis in mice by PPARalpha, beta/delta, and gamma. *J Clin Invest*. 2004; 114: 1564-76.
  44. Chawla A, Boisvert WA, Lee CH, Laffitte BA, Barak Y, Joseph SB, et al. A PPAR gamma-LXR-ABCA1 pathway in macrophages is involved in cholesterol efflux and atherogenesis. *Mol Cell*. 2001; 7: 161-71.
  45. Mandrekar S, Jiang Q, Lee CD, Koenigsnecht-Talboo J, Holtzman DM, Landreth GE. Microglia mediate the clearance of soluble A $\beta$  through fluid phase macropinocytosis. *J Neurosci*. 2009; 29: 4252-62.
  46. Romanello M, Bivi N, Pines A, Deganuto M, Quadrioglio F, Moro L, et al. Bisphosphonates activate nucleotide receptors signaling and induce the expression of Hsp90 in osteoblast-like cell lines. *Bone*. 2006; 39: 739-53.
  47. Chatterjee M, Jain S, Stuhmer T, Andrulis M, Ungethym U, Kuban RJ, et al. STAT3 and MAPK signaling maintain overexpression of heat shock proteins 90alpha and beta in multiple myeloma cells, which critically contribute to tumor-cell survival. *Blood*. 2007; 109: 720-8.
  48. Murphy LO, Blenis J. MAPK signal specificity: the right place at the right time. *Trends Biochem Sci*. 2006; 31: 268-75.
  49. Ramos JW. The regulation of extracellular signal-regulated kinase (ERK) in mammalian cells. *Int J Biochem Cell Biol*. 2008; 40: 2707-19.
  50. McKay MM, Morrison DK. Integrating signals from RTKs to ERK/MAPK. *Oncogene*. 2007; 26: 3113-21.
  51. Fourgeaud L, Traves PG, Tufail Y, Leal-Bailey H, Lew ED, Burrola PG, et al. TAM receptors regulate multiple features of microglial physiology. *Nature*. 2016; 532: 240-4.
  52. Reiserer RS, Harrison FE, Syverud DC, McDonald MP. Impaired spatial learning in the APP<sup>Swe</sup> + PSEN1<sup>DeltaE9</sup> bigenic mouse model of Alzheimer's disease. *Genes Brain Behav*. 2007; 6: 54-65.
  53. Jankowsky JL, Fadale DJ, Anderson J, Xu GM, Gonzales V, Jenkins NA, et al. Mutant presenilins specifically elevate the levels of the 42 residue beta-amyloid peptide in vivo: evidence for augmentation of a 42-specific gamma secretase. *Hum Mol Genet*. 2004; 13: 159-70.
  54. Lalonde R, Kim HD, Maxwell JA, Fukuchi K. Exploratory activity and spatial learning in 12-month-old APP(695)SWE/co+PS1/DeltaE9 mice with amyloid plaques. *Neurosci Lett*. 2005; 390: 87-92.
  55. Heneka MT, Carson MJ, Khoury JE, Landreth GE, Brosseron F, Feinstein DL, et al. Neuroinflammation in Alzheimer's disease. *Lancet Neurol*. 2015; 14: 388-405.
  56. Taipale M, Jarosz DF, Lindquist S. HSP90 at the hub of protein homeostasis: emerging mechanistic insights. *Nat Rev Mol Cell Biol*. 2010; 11: 515-28.
  57. Csermely P. Chaperone overload is a possible contributor to 'civilization diseases'. *Trends Genet*. 2001; 17: 701-4.
  58. Koren J, 3rd, Jinwal UK, Lee DC, Jones JR, Shults CL, Johnson AG, et al. Chaperone signalling complexes in Alzheimer's disease. *J Cell Mol Med*. 2009; 13: 619-30.
  59. Evans CG, Wisen S, Gestwicki JE. Heat shock proteins 70 and 90 inhibit early stages of amyloid beta-(1-42) aggregation in vitro. *J Biol Chem*. 2006; 281: 33182-91.
  60. Jinwal UK, Akoury E, Abisambra JF, O'Leary JC, 3rd, Thompson AD, Blair LJ, et al. Imbalance of Hsp70 family variants fosters tau accumulation. *FASEB J*. 2013; 27: 1450-9.
  61. Kakimura J, Kitamura Y, Takata K, Umeki M, Suzuki S, Shibagaki K, et al. Microglial activation and amyloid-beta clearance induced by exogenous heat-shock proteins. *FASEB J*. 2002; 16: 601-3.
  62. Takata K, Kitamura Y, Tsuchiya D, Kawasaki T, Taniguchi T, Shimohama S. Heat shock protein-90-induced microglial clearance of exogenous amyloid-beta1-42 in rat hippocampus in vivo. *Neurosci Lett*. 2003; 344: 87-90.
  63. Wheeler MC, Gekakis N. Hsp90 modulates PPARgamma activity in a mouse model of nonalcoholic fatty liver disease. *J Lipid Res*. 2014; 55: 1702-10.
  64. Hutchison MR, Bassett MH, White PC. SCF, BDNF, and Gas6 are regulators of growth plate chondrocyte proliferation and differentiation. *Mol Endocrinol*. 2010; 24: 193-203.
  65. Battle M, Recarte-Pelz P, Roig E, Castel MA, Cardona M, Farrero M, et al. AXL receptor tyrosine kinase is increased in patients with heart failure. *Int J Cardiol*. 2014; 173: 402-9.
  66. Axelrod H, Pienta KJ. Axl as a mediator of cellular growth and survival. *Oncotarget*. 2014; 5: 8818-52.
  67. Lemke G. Biology of the TAM receptors. *Cold Spring Harb Perspect Biol*. 2013; 5: a009076.
  68. Lai C, Lemke G. An extended family of protein-tyrosine kinase genes differentially expressed in the vertebrate nervous system. *Neuron*. 1991; 6: 691-704.
  69. Gautier EL, Shay T, Miller J, Greter M, Jakubczak C, Ivanov S, et al. Gene-expression profiles and transcriptional regulatory pathways that underlie the identity and diversity of mouse tissue macrophages. *Nat Immunol*. 2012; 13: 1118-28.
  70. Grommes C, Lee CY, Wilkinson BL, Jiang Q, Koenigsnecht-Talboo JL, Varnum B, et al. Regulation of microglial phagocytosis and inflammatory gene expression by Gas6 acting on the Axl/Mer family of tyrosine kinases. *J Neuroimmune Pharmacol*. 2008; 3: 130-40.

71. Ji R, Tian S, Lu HJ, Lu Q, Zheng Y, Wang X, et al. TAM receptors affect adult brain neurogenesis by negative regulation of microglial cell activation. *J Immunol.* 2013; 191: 6165-77.
72. Savage JC, Jay T, Goduni E, Quigley C, Mariani MM, Malm T, et al. Nuclear receptors license phagocytosis by trem2+ myeloid cells in mouse models of Alzheimer's disease. *J Neurosci.* 2015; 35: 6532-43.
73. Skerrett R, Malm T, Landreth G. Nuclear receptors in neurodegenerative diseases. *Neurobiol Dis.* 2014; 72PA: 104-16.
74. Qiu WQ, Folstein MF. Insulin, insulin-degrading enzyme and amyloid-beta peptide in Alzheimer's disease: review and hypothesis. *Neurobiol Aging.* 2006; 27: 190-8.
75. Nagele RG, D'Andrea MR, Lee H, Venkataraman V, Wang HY. Astrocytes accumulate A beta 42 and give rise to astrocytic amyloid plaques in Alzheimer disease brains. *Brain Res.* 2003; 971: 197-209.
76. Lasagna-Reeves CA, Kaye R. Astrocytes contain amyloid-beta annular protofibrils in Alzheimer's disease brains. *FEBS Lett.* 2011; 585: 3052-7.